Backstepping-Based Control of a Strapdown Boatboard Camera Stabilizer

Peyman Setoodeh, Alireza Khayatian*, and Ebrahim Farjah

Abstract: In surveillance, monitoring, and target tracking operations, high-resolution images should be obtained even if the target is in a far distance. Frequent movements of vehicles such as boats degrade the image quality of onboard camera systems. Therefore, stabilizer mechanisms are required to stabilize the line of sight of boatboard camera systems against boat movements. This paper addresses design and implementation of a strapdown boatboard camera stabilizer. A two degree of freedom (DOF) (pan/tilt) robot performs the stabilization task. The main problem is divided into two subproblems dealing with attitude estimation and attitude control. It is assumed that exact estimate of the boat movement is available from an attitude estimation system. Estimates obtained in this way are carefully transformed to robot coordinate frame to provide desired trajectories, which should be tracked by the robot to compensate for the boat movements. Such a practical robotic system includes actuators with fast dynamics (electrical dynamics) and has more degrees of freedom than control inputs. Backstepping method is employed to deal with this problem by extending the control effectiveness.

Keywords: Attitude control, attitude estimation, backstepping robot control, strapdown inertial navigation system (INS).

1. INTRODUCTION

Electro-optical sensors such as camera systems are widely used in surveillance, monitoring and searching operations. Camera systems that are mounted on vehicles such as boats are subjected to vibrations introduced by vehicle movements. These vibrations cause the line-of-sight (LOS) of the camera to shift, resulting in serious degradation of the image quality. Therefore, a camera stabilizer is required to stabilize the LOS of a boatboard camera against boat movements; rolling, pitching, and yawing. Especially in surveillance, monitoring, and target tracking operations, high stabilizing performance is needed to obtain a high-resolution image even for far targets. Rolling of the boat just turns the image plane with respect to the horizontal line and a target could still remain in the frame. Thus, compensating yawing and pitching of the boat by a pan/tilt camera stabilizer could be sufficient for target tracking. Regarding this fact, a two-degree of freedom (DOF) (yaw/pitch) robot will be able to do the task. In this paper, the controller design and the practical implementation of an LOS stabilizer for a boatboard camera is addressed. Several methods have been proposed in the literature to establish a camera stabilizing system [1].

From the mechanical structure point of view, these systems are categorized into:

- *The camera stabilization method*, which orients the camera unit directly.
- *The mirror stabilization method*, which orients a mirror to control the LOS of the camera.

From the attitude control point of view, these systems are categorized into:

- *The stable-platform system,* which is controlled directly in the inertial coordinates by measuring the inertial velocity of a camera or a mirror, mounted on a platform.
- *The Strapdown system,* which is controlled in the body base coordinates and is transformed into the inertial coordinates by measuring the vehicle's rotational movement.

In stable platform systems, camera/mirror is usually mounted on the inner axis of a multiaxis mechanical gimbal, and tracking is achieved via two servo loops. In addition to the pointing control loop, an inner stabilization or rate loop is employed to isolate the camera/mirror from platform motion. Therefore, the stabilization loop does not allow motion induced disturbances to perturb the LOS. Based on the

Manuscript received August 31, 2005; revised August 5, 2006; accepted September 7, 2006. Recommended by Editorial Board member Sangdeok Park under the direction of past Editor Keum-Shik Hong. This work was supported in part by Engineering Research Center of Fars (Shiraz, Iran).

Peyman Setoodeh, Alireza Khayatian, and Ebrahim Farjah are with the Department of Electrical Engineering, School of Engineering, Shiraz University, Zand Ave, Shiraz 7134-851154, Iran (e-mails: setoodeh@ieee.org, {khayatia, farjah}@shirazu.ac.ir).

* Corresponding author.

position of angular rate sensors, two stabilizing methods have been proposed in the literature; direct and indirect methods.

In the direct method, used for precision pointing applications, rate sensors are mounted on the LOS axes and in the indirect method, rate sensors are mounted on the gimbal base [2]. The relationships that must be considered in analyzing the design and performance of typical stabilization methods for a two-axis gimbal and a half-range mirror assembly are thoroughly discussed in [3,4]. Direct and indirect methods are analyzed and compared for LOS stabilization of a two-axis gimbaled laser tracker in [2].

Several control architectures for tow-axis gyro-stabilized mirror systems are proposed in the literature; adaptive control [5,6], H_∞ control theory [7] (chapter 12), and nonlinear robust control [8]. In [9] rate gyros are replaced by linear accelerometers and angular motion is determined from linear acceleration measurements. Control commands for the gimbal servomotors are calculated based on accelerations, and LOS stabilization is achieved by counter-rotating the imaging device. A three-axis stable platform and a two-axis hybrid motion control system aiming at a boatboard camera stabilizer are described in [1]. The proposed method in [10] uses inertial rate measurements and an adaptive feedforward filter, derived from partial inverse plant model, to cancel disturbances induced by ship motion at the base of an onboard optical telescope. The plant model is a transfer function between base disturbance inputs and tracking error. The effectiveness of the proposed method was evaluated via simulation.

Although gimbaled systems achieve lower errors than strapdown systems, they require elaborate and complex mechanical structures. Strapdown systems have simple structures and therefore they are inexpensive compared to gimbaled systems. Due to their advantages, strapdown systems are becoming widely used for different applications and stable platforms are gradually replaced by strapdown systems [11]. Despite the extensive amount of research in stable platform-based LOS stabilizers, strapdown stabilizers have received little attention in the past. This paper presents design and implementation of a strapdown boatboard camera stabilizer. Therefore the intricate design and building of the mechanical gimbals are avoided. However, strapdown system accuracy degrades quickly due to time dependent errors in inertial sensor measurements. To prevent the unbounded growth of errors, the main error sources were modeled and a sophisticated algorithm was devised to fuse inertial data with some other source of information. Therefore, it is assumed that an exact estimate of the boat movement (attitude) is available for stabilization. Attitude estimation is not the main focus of this paper and it has been reported elsewhere by the authors [12].

The main contribution of this paper is an elegant attitude compensation for a camera system, which includes all the dynamics of the camera stabilization system. This requires desired trajectory generation from attitude estimates and robot control design, which considers fast dynamics of the robot actuators.

The stabilization task will be performed by a two degree of freedom (DOF) (yaw/pitch) robot on which the camera is mounted. In practical robotic systems, actuator dynamics become really important during fast motions and should be addressed by the control schemes explicitly. Inclusion of actuators in the dynamic equations results in third-order differential equations. Therefore, the controller structure and its stability analysis is more complicated. Also, the system has more degrees of freedom than control inputs. Backstepping is a basic approach to design controllers for such systems, resulting better control effectiveness [13].

The structure of this paper is as follows. First, statement of the problem and proposed methodology is presented. Computation of desired trajectories, which should be followed by the robot joints, will be discussed later. Then backstepping-based control law with trajectory tracking is derived and validated. The paper will conclude at the final section.

2. STATEMENT OF THE PROBLEM AND PROPOSED METHODOLOGY

Consider a camera, which is mounted on a pan/tilt robot as depicted in Fig. 1, and the robot is fixed on the deck of a boat. In order to stabilize the LOS of the camera against boat movements, first the boat motion should be measured or estimated. Three coordinate frames are necessary for this purpose (Fig. 2):

- Camera frame $X^cY^cZ^c$, attached to the camera.
- body-fixed frame $X^bY^bZ^b$, fixed to the boat. Its origin usually coincides with the center of gravity and its axes coincide with the principal axes of

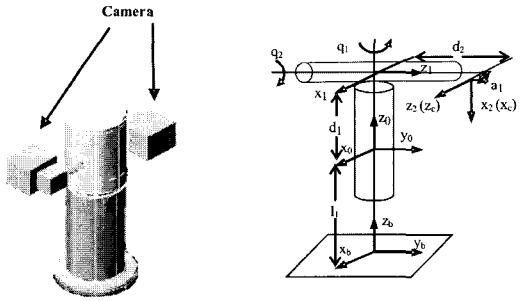

(a) (b)

Fig. 1. (a) Schematic and (b) link coordinates of the pan/tilt robot.

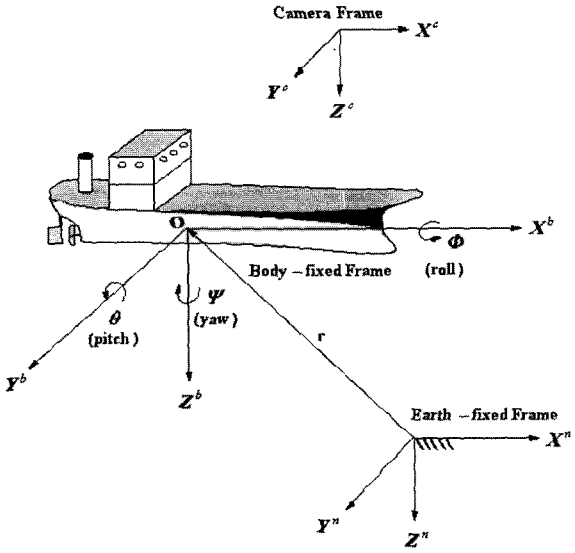

Fig. 2. Body-fixed, earth-fixed (inertial) and camera reference frames [14].

inertia.

- earth-fixed reference frame $X^nY^nZ^n$, which is a good approximation for the inertial reference frame in the case of low speed marine vehicles [14].

The motion of the body-fixed frame is described relative to the inertial reference frame. Angular velocities of the boat; ω_x, ω_y, ω_z are expressed in the body-fixed frame due to measurement of rate gyros while its orientation should be described relative to the inertial reference frame. The orientation is usually represented by Euler angles; Ψ, θ, and Φ, called yaw, pitch, and roll respectively.

Therefore, the main problem can be divided into two subproblems dealing with attitude estimation and attitude control. An attitude estimation algorithm based on an extended Kalman filter (EKF) was employed to fuse measurements of three strapdown rate gyros and some drift-free aiding sensors. Sensor fusion utilizes the complementary noise profiles of sensors to extend their limits and provide information of better accuracy and reliability [12]. It is assumed that exact estimates of the attitude are available, and the main focus of this paper is attitude control. The first step in attitude control is robot desired trajectory generation.

Desired trajectories are obtained from these estimates in such a manner that when followed by the robot joints, a coordinate frame attached to camera remains aligned with the reference frame. The second task is joint control of the robot, which should include the fast dynamics of actuators, for tracking of desired trajectories. System block diagram is shown in Fig. 3. Except for the attitude estimation block, which has been completely addressed by the authors in [12], the remaining blocks will be explained in what follows.

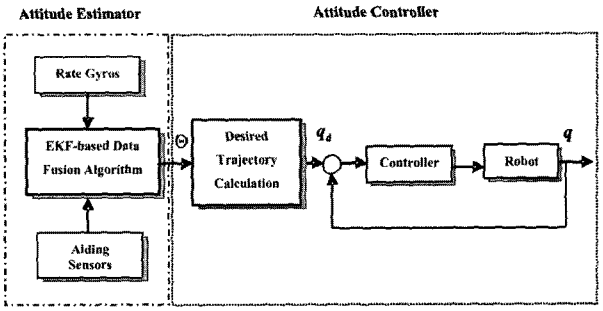

Fig. 3. System block diagram.

3. DESIRED TRAJECTORY CALCULATION

The estimated attitude is a measure of the boat rotation around each axis and should be compensated by the two DOF robot. This needs change of coordinates between reference, body and camera frames. For small angle rotations, the time rate of change of transformation from body to reference frame, $C_b^n(t)$, is governed by

$$\dot{C}_b^n = C_b^n(t)\Omega_{nb}^b, \tag{1}$$

where

$$\Omega_{nb}^b = \begin{bmatrix} 0 & -\omega_z & \omega_y \\ \omega_z & 0 & -\omega_x \\ -\omega_y & \omega_x & 0 \end{bmatrix} \tag{2}$$

is the skew-symmetric matrix formed from measurements of three strapdown rate gyros that are aligned with the body frame axes. The orientation is obtained by integrating (1), starting from a known initial orientation matrix [11].

Suppose that the two frames are initially aligned:

$$C_b^n(t=0) = I. \tag{3}$$

Integration of (1) results in:

$$C_b^n(t_{k+1}) = C_b^n(t_k)e^{\int_{t_k}^{t_{k+1}}\Omega_{nb}^b dt}, \tag{4}$$

where

$$\int_{t_k}^{t_{k+1}}\Omega_{nb}^b dt = \begin{bmatrix} 0 & -\int_{t_k}^{t_{k+1}}\omega_z dt & \int_{t_k}^{t_{k+1}}\omega_y dt \\ \int_{t_k}^{t_{k+1}}\omega_z dt & 0 & -\int_{t_k}^{t_{k+1}}\omega_x dt \\ -\int_{t_k}^{t_{k+1}}\omega_y dt & \int_{t_k}^{t_{k+1}}\omega_x dt & 0 \end{bmatrix},$$

$$\int_{t_k}^{t_{k+1}}\Omega_{nb}^b dt = \begin{bmatrix} 0 & -\Psi & \theta \\ \Psi & 0 & -\Phi \\ -\theta & \Phi & 0 \end{bmatrix} = \Theta_{nb}^b, \tag{5}$$

which is the skew-symmetric matrix formed from the attitude vector $\Theta=[\Phi \quad \theta \quad \Psi]^T$ estimated by the extended Kalman filter. Substituting (5) into (4) gives:

$$C_b^n(t_{k+1}) = C_b^n(t_k)e^{\Theta_{nb}^b}. \tag{6}$$

Approximating $e^{\Theta_{nb}^b}$ with its Taylor series expansion yields:

$$e^{\Theta_{nb}^b} = I + \Theta_{nb}^b + \frac{\left(\Theta_{nb}^b\right)^2}{2!} + \frac{\left(\Theta_{nb}^b\right)^3}{3!} + \cdots. \tag{7}$$

Substituting powers of Θ_{nb}^b into (7) leads to [11]:

$$\begin{aligned} e^{\Theta_{nb}^b} &= I \\ &+ \left\{1 - \frac{\left(\Phi^2+\theta^2+\Psi^2\right)}{3!} + \frac{\left(\Phi^2+\theta^2+\Psi^2\right)^2}{5!} - \cdots\right\}\Theta_{nb}^b \\ &+ \left\{\frac{1}{2!} - \frac{\left(\Phi^2+\theta^2+\Psi^2\right)}{4!} + \frac{\left(\Phi^2+\theta^2+\Psi^2\right)^2}{6!} - \cdots\right\}\left(\Theta_{nb}^b\right)^2. \end{aligned} \tag{8}$$

Thus, numerical integration in (1) is replaced by algebraic computation in (6).

For simplicity it is assumed that the body frame and the robot base frame are the same. To keep the robot tooltip frame or camera frame aligned with the reference frame despite the movements of the boat, the following relation must be satisfied.

$$C_b^n C_c^b = I \;\Rightarrow\; C_c^b = \left(C_b^n\right)^{-1} = \left(C_b^n\right)^T, \tag{9}$$

where C_c^b is the coordinate transformation from camera frame to the body frame and gives the desired orientation of the robot tooltip with respect to its base.

Schematic of the two DOF robot, which is employed for the LOS stabilization task, is depicted in Fig. 1(a). Two cameras are mounted on its horizontal arm, in opposite directions with respect to the robot vertical axis. This symmetrical structure leads to a constant potential energy for the robot and simplifies the dynamic model. Denavit-Hartenberg (D-H) algorithm, gives the link-coordinate diagram shown in Fig. 1(b). Regarding the kinematic model of the robot, we have:

$$C_c^b = \begin{bmatrix} \cos q_1\cos q_2 & -\sin q_1 & \cos q_1\sin q_2 \\ \sin q_1\cos q_2 & \cos q_1 & \sin q_1\sin q_2 \\ -\sin q_2 & 0 & \cos q_2 \end{bmatrix}, \tag{10}$$

where q_1 and q_2 are the joint variables depicted in Fig. 1(b). By equating (10) to $\left(C_b^n\right)^T$ we have:

$$\tan(q_1) = -\frac{\left(C_b^n\right)_{12}^T}{\left(C_b^n\right)_{22}^T}, \quad \tan(q_2) = -\frac{\left(C_b^n\right)_{31}^T}{\left(C_b^n\right)_{33}^T}. \tag{11}$$

Therefore, desired setpoints for the control loop are obtained at each sampling instant using:

$$q_{1d} = \tan^{-1}\left(-\frac{\left(C_b^n\right)_{12}^T}{\left(C_b^n\right)_{22}^T}\right), \quad q_{2d} = \tan^{-1}\left(-\frac{\left(C_b^n\right)_{31}^T}{\left(C_b^n\right)_{33}^T}\right). \tag{12}$$

Based on (12), desired accuracy points for robot joints to track are obtained from estimates of the boat movements. Suitable smooth trajectories should be generated between these accuracy points. Third order interpolating polynomial is a reasonable choice to achieve continuous velocity, and zero initial and final accelerations [15].

4. BACKSTEPPING CONTROL LAW

Backstepping is a recursive procedure that guarantees asymptotic stability by interlacing the choice of a Lyapunov function with the design of feedback control. It breaks a design problem into a sequence of design problems for lower order (even scalar) systems. Therefore, it can extend various controller design techniques to a wider class of systems by exploiting the extra flexibility that exists with lower order systems [13,16]. Backstepping-based control of rigid robots including actuators has been studied in [13,17,18].

A robot is controlled by a sequence of input voltages to its joint actuators. These control signals should guarantee stability and execution of the commanded task based on desired trajectories, while satisfying some design criteria such as transient and steady state response requirements. Backstepping method could be utilized for nonlinear position control in robotic systems. It guarantees asymptotic stability in tracking of desired position and speed trajectories, while preserving useful system nonlinearities. Also, it deals with motor electrical dynamics and extends the control effectiveness of the system [13,17]. The approach presented here is based on the controllers proposed in [17] and [18].

Dynamics of the two-link manipulator with revolute joints driven by armature-controlled DC motors, including both motor electrical and mechanical dynamics, are described by [17]:

$$\begin{cases}\left(D(q)+r^2J_m\right)\ddot{q}+\left(B(q,\dot{q})+r^2B_m\right)\dot{q}+G(q)=rK_ri \\ L\dot{i}+Ri+K_m\dot{q}=u,\end{cases} \quad (13)$$

where $q \in R^2$ is the vector of joint positions, $i \in R^2$ is the vector of armature currents and $u \in R^2$ is the vector of armature voltages; $D(q)$ is the manipulator mass matrix, which is a symmetric positive definite matrix and for the robot of Fig. 1(b), is given by:

$$D(q)=\begin{bmatrix} I_{zz}^{C1}+I_{xx}^{C2}\sin^2 q_2+I_{yy}^{C2}\cos^2 q_2+I_{xy}^{C2}\sin(2q_2) & I_{yz}^{C2}\cos q_2-I_{xz}^{C2}\sin q_2 & I_{yz}^{C2}\cos q_2-I_{xz}^{C2}\sin q_2 \\ & & I_{zz}^{C2}\end{bmatrix}, \quad (14)$$

where I^{Cj} is the matrix of moments of inertia of link j with respect to its center of mass. $B(q,\dot{q})\dot{q}$ represents the centripetal and Coriolis forces and is given by:

$$B(q,\dot{q})=\begin{bmatrix} \dot{q}_2\left(I_{xx}^{C2}\sin(2q_2)-I_{yy}^{C2}\sin(2q_2)+2I_{xy}^{C2}\cos(2q_2)\right) \\ -\frac{1}{2}\dot{q}_1\left((I_{xx}^{C2}-I_{yy}^{C2})\sin(2q_2)+2I_{xy}^{C2}\cos(2q_2)\right) \\ -\dot{q}_2\left(I_{yz}^{C2}\sin q_2+I_{xz}^{C2}\cos q_2\right) \\ 0\end{bmatrix}. \quad (15)$$

$G(q)$ denotes the gravitational force, which due to the symmetrical structure of the system, its elements are zero. J_m is the actuator inertia matrix, B_m is the diagonal matrix of damping terms, L represents the actuator inductance matrix, R is the actuator resistance matrix, K_m is the matrix characterizing the voltage constant of the actuator, K_r is the matrix which characterizes the electromechanical conversion between current and torque, and r is the gear ratio matrix. It is assumed that $\dot{q}$, q, and i are measurable [17,18].

Following the notation of [17], state vectors of positions q, speeds $\dot{q}$, and currents i, are chosen as:

$$\xi_2=\dot{q}=\begin{bmatrix}\dot{q}_1 & \dot{q}_2\end{bmatrix}^T, \quad \xi_1=q=\begin{bmatrix}q_1 & q_2\end{bmatrix}^T,$$
$$\xi=\begin{bmatrix}\xi_1 & \xi_2\end{bmatrix}^T, \quad (16)$$
$$\xi_3=i=\begin{bmatrix}i_1 & i_2\end{bmatrix}^T, \quad (17)$$

where $\xi \in R^4$ and $\xi_3 \in R^2$. For simplicity of the notation, $D(q)+r^2J_m$ and $B(q,\dot{q})+r^2B_m$ are called $M(q)$ and $C(q,\dot{q})$, respectively.

The objective is to find a control law u to stabilize the state of the system (13). To ensure the asymptotic stability of the system, considering a given output, the backstepping technique fixes a storage function and calculates the Lyapunov candidate and stabilizing functions. Consider the output:

$$y=(\xi_3-\xi_{3d})-\alpha_0(\xi), \quad (18)$$

the Lyapunov candidate function:

$$V(\xi,\xi_3)=W(\xi)+\frac{1}{2}y^Ty, \quad (19)$$

the storage function:

$$W(\xi)=\frac{1}{2}(\xi_1-\xi_{1d})^T(\xi_1-\xi_{1d}), \quad (20)$$

and the stabilization function:

$$\alpha_0(\xi)=(\xi_3-\xi_{3d})-(\xi_2-\xi_{2d}). \quad (21)$$

Implying the limit $\dot{V}(\xi,\xi_3) \le -y^Ty$, yields the final backstepping control law as [17]:

$$\begin{aligned}u=L\Big(&L^{-1}(R\xi_3+K_m\xi_2)+\dot{\xi}_{3d}-(\xi_2-\xi_{2d}) \\ &-(\xi_1-\xi_{1d})+M^{-1}(\xi_1)C(\xi_1,\xi_2)\xi_2 \\ &+M^{-1}(\xi_1)G(\xi_1)-M^{-1}(\xi_1)rK_r\xi_3\Big).\end{aligned} \quad (22)$$

If all the parameters are known, in addition to the desired position, velocity, and acceleration trajectories, derivative of the desired current, $\dot{\xi}_{3d}$, is also required. Desired current, ξ_{3d}, can be obtained by substituteing of desired position, velocity, and acceleration in (13).

To calculate ξ_{3d} and $\dot{\xi}_{3d}$, the model (13) could be written as:

$$\begin{cases}M(q)\ddot{q}+C(q,\dot{q})\dot{q}+G(q)=rK_ri_d+rK_r\tilde{i} \\ L\dot{i}+Ri+K_m\dot{q}=u,\end{cases} \quad (23)$$

where $\tilde{i}$ is current error. Then the manipulator can be regarded as a subsystem, which is derived by two inputs; the control command, K_ri_d, and disturbance, $K_r\tilde{i}$. Using the state variables in (16) and (17), desired current vector and its derivative can be calculated from (23) as:

$$\begin{aligned}\xi_{3d}=(rK_r)^{-1}\Big(&M(\xi_{1d})\dot{\xi}_{2d}+C(\xi_{1d},\xi_{2d})\xi_{2d} \\ &+G(\xi_{1d})-K_d\varepsilon\Big),\end{aligned} \quad (24)$$

$$\begin{aligned}\dot{\xi}_{3d}=(rK_r)^{-1}\Big(&M(\xi_{1d})\ddot{\xi}_{2d}+C(\xi_{1d},\xi_{2d})\dot{\xi}_{2d} \\ &+\dot{M}(\xi_{1d})\dot{\xi}_{2d}+\dot{C}(\xi_{1d},\xi_{2d})\xi_{2d} \\ &+\dot{G}(\xi_{1d})-K_d\dot{\varepsilon}\Big),\end{aligned} \quad (25)$$

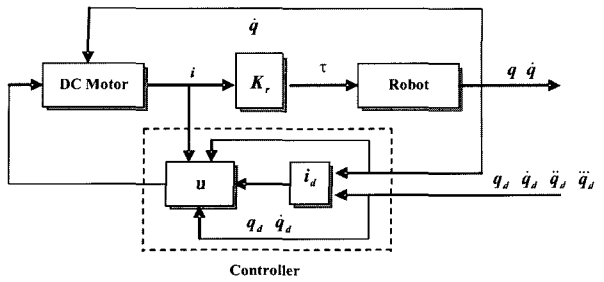

Fig. 4. Robot system and controller block diagram [17].

where ε is the error given by:

$$\varepsilon = \xi_2 - \xi_{2d} - \Lambda(\xi_1 - \xi_{1d}) \tag{26}$$

and Λ is a positive definite diagonal matrix [17].

Fig. 4 depicts the block diagram of the system (13) and the controller (22). The dynamic model (13) consists of two subsystems; the manipulator and the actuator. These are related to the first and second equations in (13), respectively. The torque $K_r i$, which is the input of the manipulator dynamics, can not be synthesized directly because it is the output of the actuator dynamics. Therefore the controller consists of two parts and the control command is calculated in two steps:

- The armature current vector, i, is regarded as the control variable for the manipulator subsystem. An embedded control input, i_d, is designed to guarantee the convergence of tracking error in the absence of actuator dynamics.
- The armature voltage vector, u, is regarded as the control variable for the actuator subsystem and provides desired motions. In other words, it forces $q(t)$ to track $q_d(t)$ by regulating the real armature currents i about the embedded currents i_d.

The recursive nature of the backstepping method guarantees the global stability of the closed loop system [18].

5. RESULTS

This section presents the performance evaluation of the proposed backstepping based controller for the application at hand. The two DOF (pan/tilt) robot parameters are listed in Table 1. The robot actuators are two 24-volt DC servomotors with the characteristics listed in Table 2. The rotation of the robot joints are measured by rotary optical encoders. Low-cost low-accuracy RG18A rate gyros, PENDL2A gravimetric inclinometers, and a magnetic compass are employed in the testbed for attitude estimation [12]. A Pentium II-233 MHz computer is used to control the robot via a PCL-832 3-axis servomotor control card by pulse width modulation (PWM) signals. PCL-832 provides a simulated tachometer output and therefore reduces the overall cost. The required subroutines are written in standard C language.

Table 1. Robot parameters.

ℓ_1 (The z component of the center of mass of link 1 in the base coordinate frame)	0.546m
d_1 (The z component of the center of mass of link 2 in coordinate frame 0)	0.980m
d_2 (The z component of the center of camera coordinate frame in coordinate frame 1)	0.280m
a_1 (The x component of the center of camera coordinate frame in coordinate frame 1)	0.040m
I^{C_1} (The matrix of moments of inertia of link 1 with respect to its center of mass)	$\begin{bmatrix} 4.0088 & 0.0124 & 0.0469 \\ 0.0124 & 4.4970 & 0.0092 \\ 0.0469 & 0.0092 & 2.5414 \end{bmatrix}$ Kg·m^2
I^{C_2} (The matrix of moments of inertia of link 2 with respect to its center of mass)	$\begin{bmatrix} 0.1104 & 0 & -0.0116 \\ 0 & 0.1117 & 0 \\ -0.0116 & 0 & 0.0074 \end{bmatrix}$ Kg·m^2

Table 2. Servomotor parameters.

Motor No.	K_r (Nm/A)	K_m (rpm/volt)	R (Ohm)	L (mH)	J_m (Kg.m^2)	B_m (N.s)	*Gear ratio* (r)
1	2.7	119	0.176	0.08	1.460e-004	0.2276	92.7:1
2	0.274	25.6	0.4695	0.04	1.000e-004	0.0721	5.6:1

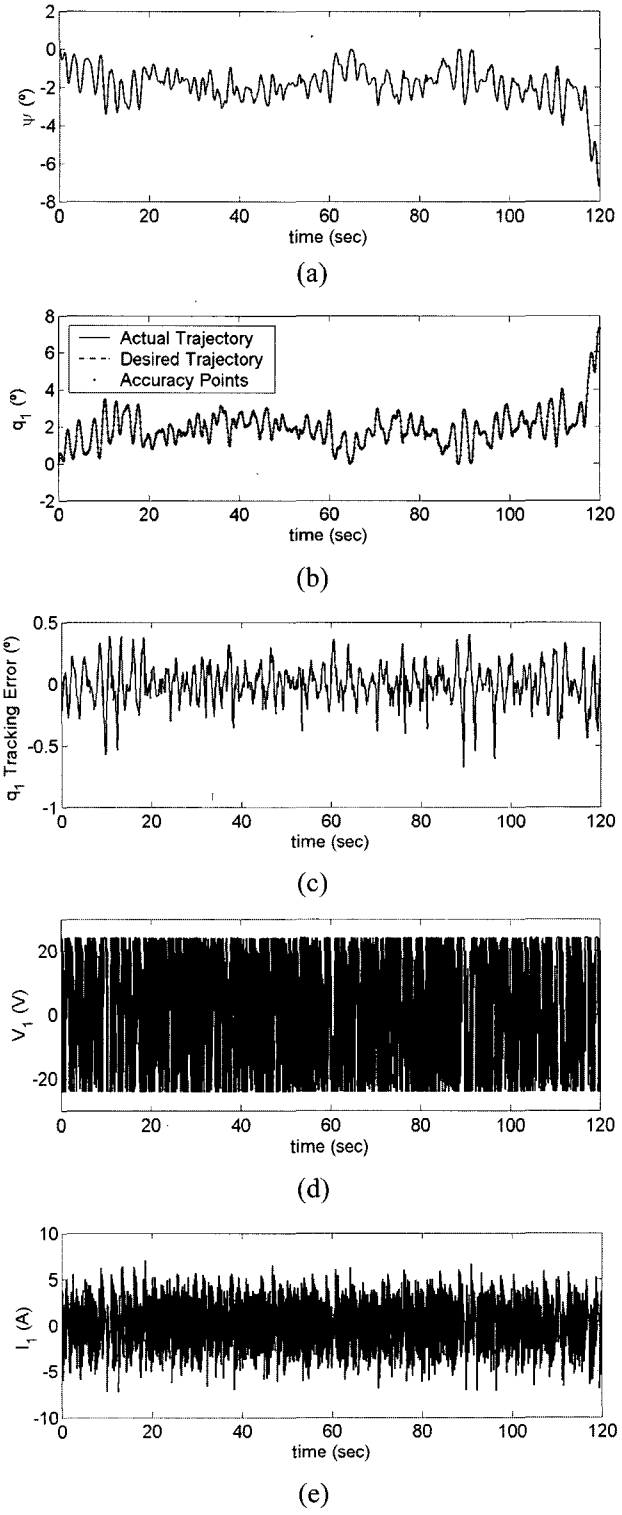

Fig. 5. Trajectory tracking results for yaw angle: (a) estimation of the boat orientation (b) desired and actual trajectories (c) tracking error (d) voltage and (e) current of the first actuator.

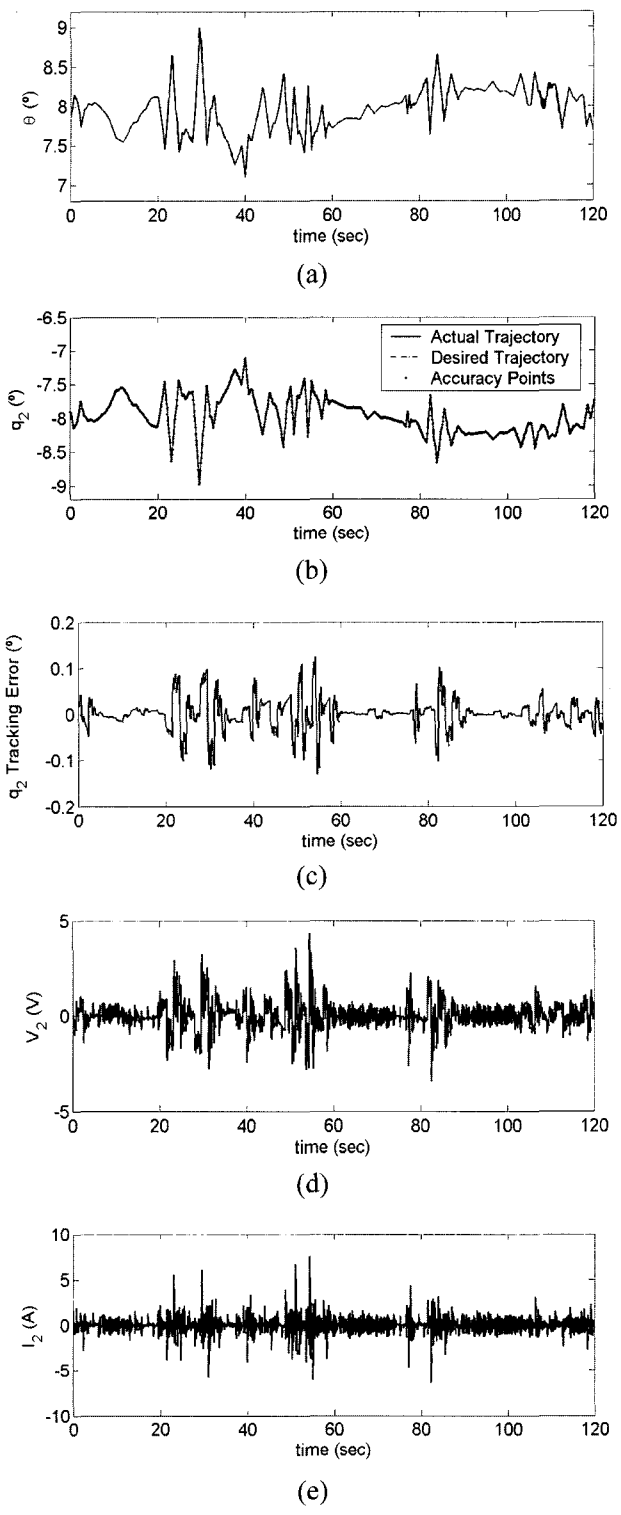

Fig. 6. Trajectory tracking results for pitch angle: (a) estimation of the boat orientation (b) desired and actual trajectories (c) tracking error (d) voltage and (e) current of the second actuator.

Due to the parameter values of Table 2, the electrical time constants (L/R) and mechanical time constants (J/B) are respectively 0.45 and 0.64 msec for the first actuator and 0.085 and 1.38 msec for the second actuator. The electrical time constant of second actuator is much smaller than its mechanical time constant. This leads to a reduced order model of the actuator dynamics. But the same assumption is not

valid for the first actuator because its electrical and mechanical time constants are of the same order. Thus, the electrical dynamics are not negligible and must be included in the system dynamics. The electrical time constant produce high frequency dynamics that must be addressed in controller design. The backstepping technique can solve this problem.

As the time constant of a buoyant boat is about 0.2~0.3 seconds, a 10Hz sampling rate was chosen for attitude estimator to satisfy the sampling theorem [12]. To evaluate the performance of the designed controller one sample dataset for a period of 120 seconds, recorded on the sea surface, is presented for yaw and pitch channels. The output of the attitude estimator, which is the estimation of the boat movement, is shown in Fig. 5(a) and 6(a) for yaw and pitch angles, respectively in the test period. Desired trajectories are generated from these orientation estimates. Then the control commands are computed based on these trajectories and are exerted each 10 msec. The actual trajectories followed by the robot joints and the corresponding desired trajectories are plotted against time in Fig. 5(b) and 6(b). Fig. 5(c) and 6(c) depict the tracking error during the test period. Voltage and current of the actuators are shown in Fig. 5(d), 5(e), 6(d), and 6(e), which reveals that the controller is implementable. These results show the tracking capability of the backstepping controller with reasonable control effort.

The chattering problem in the voltage waveforms in Figs. 5 and 6 is partly because of the differential terms and perturbations, and partly because of the severity of the trajectories, which causes the saturation of the actuators. However, as mentioned in [18] and [19], the torque signal is smoother than the voltage signal after a low pass filtering of the motor dynamics. Also, the servomotors are controlled by PWM signals. Therefore, the chattering voltage will be less problematic from a practical point of view.

In order to reduce the chattering problem, severe trajectories have to be scaled dynamically at the expense of control accuracy [15]. Moreover, modified versions of the backstepping algorithm such as [20], are promising for chattering reduction, which is a subject for our future research.

To show the advantage of the proposed algorithm and justify for using the third order model, which includes the actuator dynamics, its performance is compared with the torque-level inverse dynamics controller, which is based on the second order model [15]. Semi-experiments were performed by using the desired trajectories obtained from the attitude estimator based on the data collected on the sea surface in the previous experiment, as the reference signal for the inverse dynamics controller. Tracking errors for both controllers are compared in Fig. 7, which shows the superior performance of the backstepping controller.

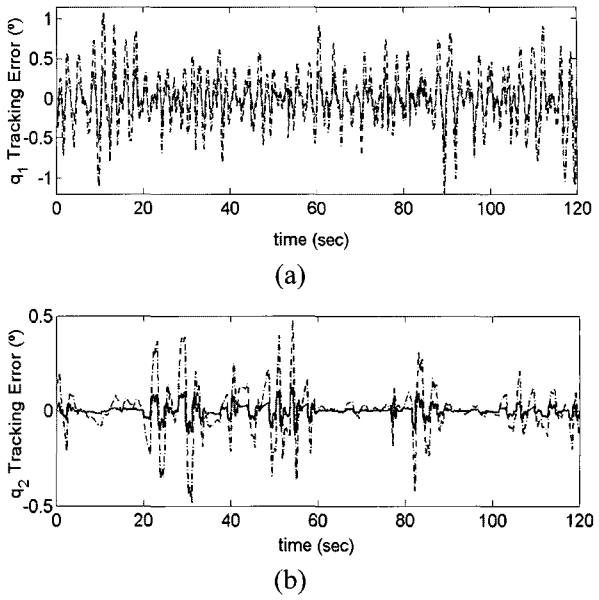

Fig. 7. Tracking error for (a) yaw angle (b) pitch angle; solid line: backstepping voltage-level control, dash-dot line: inverse dynamics torque-level control.

6. CONCLUSION

In this paper a backstepping-based control law was used to stabilize the line of sight of a boatboard camera mounted on a two DOF robot. The controller incorporates both manipulator and actuator electrical and mechanical dynamics and allows preserving all nonlinearities of the system. The control law requires the measurement of joint positions, velocities and motor armature currents and addresses the problem of fast dynamics of actuators. Asymptotic stability of the closed loop system is established in the Lyapunov sense. The results obtained for position control problem are rather encouraging and the control effort is reasonable.

REFERENCES

[1] J. Takiguchi, K. Nojima, and K. Iwama, "Development of a boatboard infra-red camera stabilizer," *Proc. of the 4th Conference on Motion and Vibration Control*, MOVIC'98, 1998.

[2] P. J. Kennedy and R. L. Kennedy, "Direct versus indirect line of sight (LOS) stabilization," *IEEE Trans. on Control Systems Technology*, vol. 11, no. 1, pp. 3-15, January 2003.

[3] A. K. Rue, "Stabilization of precision electro-optical pointing and tracking systems," *IEEE Trans. on Aerospace & Electronic Systems*, vol. 5, pp. 805-819, September 1969.

[4] A. K. Rue, "Precision stabilization systems,"

IEEE Trans. on Aerospace & Electronic Systems, vol. 10, no. 1, pp. 34-42, January 1974.

[5] T. H. Lee, E. K. Koh, and M. K. Loh, "Stable adaptive control of multivariable servo-mechanisms, with application to a passive line-of-sight stabilization system," *IEEE Trans. on Industrial Electronics*, vol. 43, no. 1, pp. 98-105, February 1996.

[6] T. H. Lee, K. K. Tan, A. Mamun, M. W. Lee, and C. J. Khoh, "Composite control of gyro mirror line-of-sight stabilization platform - design and auto-tuning," *Proc. of the 13th World Congress on Intelligent Control and Automation*, pp. 3150-3155, 2000.

[7] B. M. Chen, *H_∞ Control and its Applications*, Springer-Verlag, 1998.

[8] H. Ambrose, Z. Qu, and R. Johnson, "Nonlinear robust control for a passive line-of-sight stabilization system," *Proc. of IEEE Conference on Control Applications*, pp. 942-947, 2001.

[9] M. C. Algrain and J. Quinn, "Accelerometer based line of sight stabilization approach for pointing and tracking systems," *Proc. of IEEE Conference on Control Applications*, pp. 159-163, 1993.

[10] M. A. Borrello, D. Leslie, and H. Hyman, "Shipboard disturbance control for the rapid optical beam steering (ROBS) pointing and tracking system," *Proc. of American Control Conference*, pp. 3186-3190, 2002.

[11] D. H. Titterton and J. L.Weston, *Strapdown Inertial Navigation Technology*, 2nd edition, AIAA, 2004.

[12] P. Setoodeh, A. Khayatian, and E. Farjah, "Attitude estimation by separate-bias Kalman filter-based data fusion," *The Journal of Navigation*, vol. 57, no. 2, pp. 261-273, May 2004.

[13] F. L. Lewis, S. Jagannathan, and A. Yesidirek, *Neural Network Control of Robot Manipulators and Nonlinear Systems*, Taylor & Francis Ltd., 1999

[14] T. I. Fossen, *Guidance and Control of Ocean Vehicles*, John Wiley & Sons, 1994.

[15] L. Sciavicco and B. Siciliano, *Modeling and Control of Robot Manipulators*, 2nd edition, Springer-Verlag, 2000.

[16] H. K. Khalil, *Nonlinear Systems*, 2nd ed., Prentice-Hall, 1996.

[17] D. Nganga-Kouya, M. Saad, L. Lamarche, and C. Khairallah, "Backstepping adaptive position control for robotic manipulators," *Proc. of American Control Conference*, pp. 636-640, 2001.

[18] C. Y. Su and Y. Stepaneneko, "Backstepping-based hybrid adaptive control of robot manipulators incorporating actuator dynamics," *International Journal of Adaptive Control and Signal Processing*, vol. 11, no. 2, pp. 141-153, March 1997.

[19] H. Sira-Ramirez, "On the dynamical sliding mode control of nonlinear systems," *International Journal of Control*, vol. 57, no. 5, pp. 1039-1061, 1993.

[20] H. G. Tanner and K. J. Kyriakopoulos, "Backstepping for nonsmooth systems," *Automatica*, vol. 39, no. 7, pp. 1259-1265, July 2003.

Peyman Setoodeh received the B.Sc. and M.Sc. degrees both in Electrical Engineering from Shiraz University, Shiraz, Iran in 1996 and 2002, respectively. He is currently working toward a Ph.D. degree in the Adaptive Systems Lab, Department of Electrical and Computer Engineering, McMaster University, Hamilton, Canada. His research interests include cognitive machines, systems biology, and complex adaptive systems.

Alireza Khayatian received the B.Sc. degree in Electrical Engineering from Isfahan Technical University, Iran in 1985, and the M.Sc. degree also in Electrical Engineering from Tarbiat Modarres University, Iran in 1988. He has been a Research Assistant in the Electromechanical Systems Laboratory at the Georgia Institute of Technology, where he received the Ph.D. degree in Control Engineering in 1993. Since 1993, he has been a Faculty Member with the Department of Electrical Engineering, Shiraz University, Shiraz, Iran and his research interests include nonlinear control, estimation and robotics.

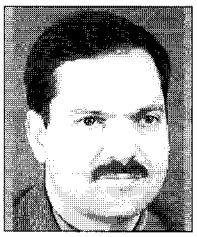

Ebrahim Farjah obtained the B.Sc. degree in Electrical and Electronics Engineering from Shiraz University, Shiraz-Iran in 1987, the M.Sc. degree in Electrical Power Engineering from Sharif University of Technology in 1989, Tehran-Iran, and the Ph.D. degree in Electrical Engineering from INPG, Grenoble-France. He is currently an Assistant Professor in the EE department of Shiraz University. His research field includes electrical machines drive and power electronics.